Polymeric synthetic nanoparticles for the induction of antigen-specific immunological tolerance

Roberto A. Maldonado[a], Robert A. LaMothe[a], Joseph D. Ferrari[a], Ai-Hong Zhang[b], Robert J. Rossi[b], Pallavi N. Kolte[a], Aaron P. Griset[a], Conlin O'Neil[a], David H. Altreuter[a], Erica Browning[a], Lloyd Johnston[a], Omid C. Farokhzad[c,d], Robert Langer[e,f], David W. Scott[b], Ulrich H. von Andrian[g,h], and Takashi Kei Kishimoto[a,1]

[a]Selecta Biosciences, Inc., Watertown, MA 02472; [b]Department of Medicine, Uniformed Services University of the Health Sciences, Bethesda, MD 20814; [c]Laboratory of Nanomedicine and Biomaterials, Department of Anesthesiology, Brigham and Women's Hospital, Harvard Medical School, Boston, MA 02115; [d]King Abdulaziz University, Jeddah 22254, Saudi Arabia; [e]Department of Chemical Engineering, Massachusetts Institute of Technology, Cambridge, MA 02139; [f]The David H. Koch Institute for Integrative Cancer Research, Cambridge, MA 02139; [g]Division of Immunology, Department of Microbiology and Immunobiology, Harvard Medical School, Boston, MA 02115-6017; and [h]The Ragon Institute of Massachusetts General Hospital, Massachusetts Institute of Technology and Harvard, Cambridge, MA 02139

Edited by Robert L. Coffman, Dynavax Technologies, Berkeley, CA, and approved November 6, 2014 (received for review May 10, 2014)

Current treatments to control pathological or unwanted immune responses often use broadly immunosuppressive drugs. New approaches to induce antigen-specific immunological tolerance that control both cellular and humoral immune responses are desirable. Here we describe the use of synthetic, biodegradable nanoparticles carrying either protein or peptide antigens and a tolerogenic immunomodulator, rapamycin, to induce durable and antigen-specific immune tolerance, even in the presence of potent Toll-like receptor agonists. Treatment with tolerogenic nanoparticles results in the inhibition of CD4+ and CD8+ T-cell activation, an increase in regulatory cells, durable B-cell tolerance resistant to multiple immunogenic challenges, and the inhibition of antigen-specific hypersensitivity reactions, relapsing experimental autoimmune encephalomyelitis, and antibody responses against coagulation factor VIII in hemophilia A mice, even in animals previously sensitized to antigen. Only encapsulated rapamycin, not the free form, could induce immunological tolerance. Tolerogenic nanoparticle therapy represents a potential novel approach for the treatment of allergies, autoimmune diseases, and prevention of antidrug antibodies against biologic therapies.

nanoparticles | immune tolerance | rapamycin | immunotherapy | anti-drug antibodies

Undesired immunogenicity can have a profound impact on human health. Allergies, including allergic asthma and severe food allergies, affect ∼20% of the population, and the prevalence has been steadily increasing over the past several decades (1). The prevalence of autoimmune diseases, including multiple sclerosis and type 1 diabetes, is ∼4.5% (2). Unwanted immunogenicity can also affect both efficacy and safety of biologic drugs (3), particularly in the case of protein replacement therapies for the treatment of genetic deficiencies, such as hemophilia A (4) and Pompe Disease (5). Immunomodulatory agents commonly used to control immunogenicity are often broadly immunosuppressive and typically require chronic administration that can lead to reactivation of latent pathogens, development of tumors, and opportunistic infections (6, 7). Therefore, antigen-specific, durable tolerogenic therapy would be highly desirable from an efficacy and safety perspective.

Multiple techniques for antigen-specific immunotherapy have been described, although only allergen immunotherapy, wherein low doses of antigen are delivered in the absence of immunomodulating agents, is currently used in the clinic (1). Experimental approaches have included oral administration of antigen, high dose tolerance, and the use of altered peptide ligands (8). Although these methods have been successful in preclinical models, translation to human clinical trials has been largely disappointing (8). Alternative strategies to leverage tolerogenic programming associated with apoptotic cells include conjugating antigen to splenocytes (9–12) or synthetic microparticles (13, 14) or targeting antigen to the surface of red blood cells (15). Other approaches include loading particles with MHC complexes that present relevant peptides in the absence of costimulation (16, 17), liposomal copresentation of antigen with a ligand specific for the negative signaling receptor CD22 on B cells (18), codelivery of peptide antigen with an aryl hydrocarbon receptor agonist (19), and cotreatment with pharmacological agents, such as methotrexate (20). A major concern for antigen immunotherapy is the ability to induce and maintain tolerance in the presence of proinflammatory stimuli caused by tissue stress, injury, or concurrent infections. We sought to develop an antigen-specific tolerogenic technology that could control both T-cell– and B-cell–mediated immunity and that was durable over time and to multiple challenges with the antigen, even in the presence of strong innate immune stimulants.

Dendritic cells (DCs) are an attractive target for immunotherapies due to their central role in antigen presentation to T cells and their ability to induce and control regulatory responses

Significance

Synthetic nanoparticles containing either protein or peptide antigen and the immunosuppressant rapamycin are capable of inducing durable and specific resistance to mounting immune responses toward the antigen. This immunological tolerance operates on lymphocytes even after multiple immunogenic challenges with the antigen and adding enhancers of immune responses (adjuvants). As a result, the animals treated with these tolerogenic nanoparticles (tNPs) show reduced allergic hypersensitivity disorders, protection from disease relapse in a model of multiple sclerosis, and prevention of inhibitory antidrug antibody responses in an animal model of hemophilia A. These results show the potential for nanocarriers to modify the immunoreactivity of a given molecule by providing tolerogenic instructions to the immune system, thereby preventing or reversing pathological and neutralizing immune responses.

Author contributions: R.A.M., R.A.L., J.D.F., A.-H.Z., D.W.S., U.H.v.A., and T.K.K. designed research; R.A.M., R.A.L., J.D.F., A.-H.Z., R.J.R., P.N.K., A.P.G., C.O., D.H.A., and E.B. performed research; A.P.G., C.O., D.H.A., L.J., O.C.F., and R.L. contributed new reagents/analytic tools; R.A.M., R.A.L., J.D.F., A.-H.Z., R.J.R., P.N.K., A.P.G., C.O., D.H.A., E.B., L.J., O.C.F., D.W.S., U.H.v.A., and T.K.K. analyzed data; and R.A.M. and T.K.K. wrote the paper.

Conflict of interest statement: U.H.v.A., O.C.F., and R.L. are co-founders and shareholders of Selecta Biosciences. The other authors—except for D.W.S., A.-H.Z., and R.J.R.—are employees and shareholders of Selecta Biosciences. D.W.S. received financial support from Selecta Biosciences.

This article is a PNAS Direct Submission.

Freely available online through the PNAS open access option.

[1]To whom correspondence should be addressed. Email: kkishimoto@selectabio.com.

This article contains supporting information online at www.pnas.org/lookup/suppl/doi:10.1073/pnas.1408686111/-/DCSupplemental.

to secure self-tolerance (21–25). Thomson and colleagues (26, 27) demonstrated that treating DCs with rapamycin, an inhibitor of the mTOR pathway, induces a tolerogenic DC phenotype capable of inducing Treg differentiation and antigen-specific immune tolerance that is resistant to the proinflammatory cascade triggered by TLR signaling. However, conventional therapy with free rapamycin requires chronic systemic administration, resulting in broad immunosuppression due to its direct effect on lymphocytes (28), whereas low doses of rapamycin may paradoxically augment effector T-cell memory (29). Thus, it would be desirable to transiently target rapamycin's effects to DCs and other antigen-presenting cells (APCs) at the time of antigen encounter. Nanoparticles (NPs) are an ideal mechanism to deliver antigen (16, 30, 31) and drugs (32) to APCs, as these cells are keyed to capture and internalize nanoparticulates such as viruses.

Here we describe the development of tolerogenic NPs (tNPs) using materials and compounds that have been well validated in the clinic. These self-assembling, biodegradable poly(lactide-coglycolide) (PLGA) tNPs containing either protein or peptide antigens and rapamycin are capable of inducing durable antigen-specific tolerance that control adaptive immune responses and withstand multiple immunogenic challenges with antigen. We demonstrate that either s.c. or i.v. administration of tNPs inhibits the activation of antigen-specific CD4+ and CD8+ T cells and B cells while inducing antigen-specific Tregs and Bregs. Swiss Jack Lambert (SJL) mice immunized with the myelin proteolipid protein 139–151 peptide in complete Freud's adjuvant ($PLP_{139–151}$/CFA) and treated therapeutically with a single dose of tNPs at the peak of disease are completely protected from developing relapsing paralysis. In hemophilia A animals, administration of tNP before or after the establishment of an anti-factor VIII (FVIII) antibody response led to a significant reduction of the neutralizing antibody response against FVIII. Treatment of mice with tNP prevents both cellular and humoral immunity even in the presence of potent TLR agonists. These effects are dependent on the presence of the encapsulated rapamycin (not free in solution).

Results

Induction of CD4+ T-Cell Tolerance Using tNPs. PLGA tNPs containing rapamycin and chicken ovalbumin (OVA) or rapamycin and the MHC class II-restricted OVA peptide 323–339 ($OVA_{323–339}$) were prepared using a water-in-oil-in-water double emulsion process (Fig. 1*A*). To investigate whether tNPs could inhibit CD4+ T-cell activation, T cells specific for the $OVA_{323–339}$ peptide (OTII T cells) were adoptively transferred into naive animals. Mice were then immunized s.c. with $OVA_{323–339}$ admixed with a TLR7/8 agonist, R848, and concomitantly treated i.v. with tNP or control NPs. Four days postimmunization, the number of OTII T cells in the draining popliteal lymph node (popLN) of animals that were immunized but not treated was ~6.5-fold greater than that of their naïve, unimmunized counterpart (Fig. 1*B*). The i.v. administration of tNPs completely abrogated the proliferation of OTII T cells, whereas empty NPs admixed with $OVA_{323–339}$ peptide had little effect. Of note, in these experiments, the tNP treatment was administered i.v., whereas the immunization was provided locally by s.c. administration. To test the direct, local effect of tNP treatment, subsequent experiments evaluated s.c. administration of tNPs (Fig. 1*C*). Control NPs containing $OVA_{323–339}$ only (NP[$OVA_{323–339}$]) induced the activation and proliferation of OTII T cells in the draining popLN, whereas no expansion was observed after treatment with tNP containing rapamycin and $OVA_{323–339}$. However, an increase in the percentage of Foxp3+CD25+ OTII T cells was evident after tNP treatment, indicating induction of T regulatory cells. Unexpectedly, the opposite trends were observed when an equivalent amount of free rapamycin (10 μg) was admixed with NP [$OVA_{323–339}$] (Fig. 1*C*). These results suggest that administration of tNP led to the formation of MHC class II-restricted regulatory T cells that inhibited the activation of CD4 T-cell immunity and that codelivery of antigen with encapsulated rapamycin was critical. To avoid the possible direct suppressive activity of residual encapsulated rapamycin on CD4 T-cell activation, mice were treated i.v. with tNP 6 d before the OTII T-cell transfer to allow time for the inhibitory effect of rapamycin to dissipate (Fig. 1*D*). Immunized animals without previous treatment showed robust accumulation of the OTII T cells following immunization with free $OVA_{323–339}$+R848 s.c. (Fig. 1*D*). Treatment of mice with tNP before OTII T-cell transfer and immunization inhibited the subsequent expansion of OTII T cells, whereas injections of control NPs containing rapamycin only (NP[Rapa]) had little to no effect. These results indicate that administration of tNP can suppress CD4+OTII T-cell responses through the induction of endogenous MHC class II-restricted suppressive cells.

Inhibition of Humoral Immunity by tNP. We next investigated the effect of tNP treatment during the development of a humoral response. Mice immunized s.c. with an admix of OVA and a TLR9 agonist, CpG oligonucleotides (OVA+CpG), showed a mounting antibody response with increasing anti-OVA titers with each successive boost (Fig. 2 *A* and *B*). Concomitant treatment with tNP administered either s.c (Fig. 2*A*) or i.v. (Fig. 2*B*) inhibited the anti-OVA antibody response, even when the tNPs were admixed with CpG (Fig. 2*A*). The inhibition of the humoral response was dependent on the encapsulation of rapamycin, as providing the $OVA_{323–339}$ peptide alone in free or encapsulated form (NP[$OVA_{323–339}$]) or just free rapamycin (all admixed to OVA+CpG) did not affect the anti-OVA response (Fig. 2*A*). Importantly, both peptide- and protein-containing tNPs were similarly efficacious (Fig. 2*B*, *Left* and *Middle* panels, respectively). In contrast, control NP[OVA] administered s.c. or i.v. enhanced the humoral response (Fig. 2*B*, *Right*).

We next evaluated splenic B-cell activation and function in mice immunized i.v. with an immunogenic particulate form of OVA (pOVA). Approximately 10–12% of B cells (B220+) found in the local draining LN acquired a typical germinal center phenotype, expressing low levels of IgD, high levels of GL7, and the proliferation marker Ki67 (Fig. 2*C*). In contrast, when animals were concomitantly administered tNP (containing rapamycin+$OVA_{323–339}$) s.c., the proportion of activated germinal center B cells was similar to or below the levels found in naïve animals. To determine the impact of tNP treatment directly on B cells, B cells from MD4 B-cell receptor (BCR) transgenic animals were adoptively transferred into CD45.1+ animals. The transgenic BCR is specific for hen egg lysozyme (HEL), and the presence of this protein results in cell activation of MD4 B cells in vivo and in vitro (33). HEL-only particles injected i.v. induced the activation of MD4 B cells in the spleen 4 d later, however providing tNP containing similar amounts of HEL (together with rapamycin) did not (Fig. 2*D*). These results show that treatment with tNP inhibited B-cell activation and differentiation into antibody-producing cells.

Durability of the tNP Treatment Effect. Mice were injected s.c. with tNP or saline admixed with OVA+CpG (days 0, 14, and 28) and OVA (days 42, 56, 70, 84, and 98; Fig. 3*A*). Animals treated concurrently with tNPs showed a substantial delay in the development of anti-OVA antibodies, and the titers remained ~37-fold lower than those observed in the immunized controls. Of the 53 animals that were treated with tNP (nine independent experiments), 15 showed no detectable titers and 38 showed low titers at days 91–119 compared with animals in the untreated group (*Inset* table in Fig. 3*A*). Only three animals (5%) of tNP-treated animals showed titers greater than 2,000, compared with 59 animals (92%) in the control group. To test the durability of

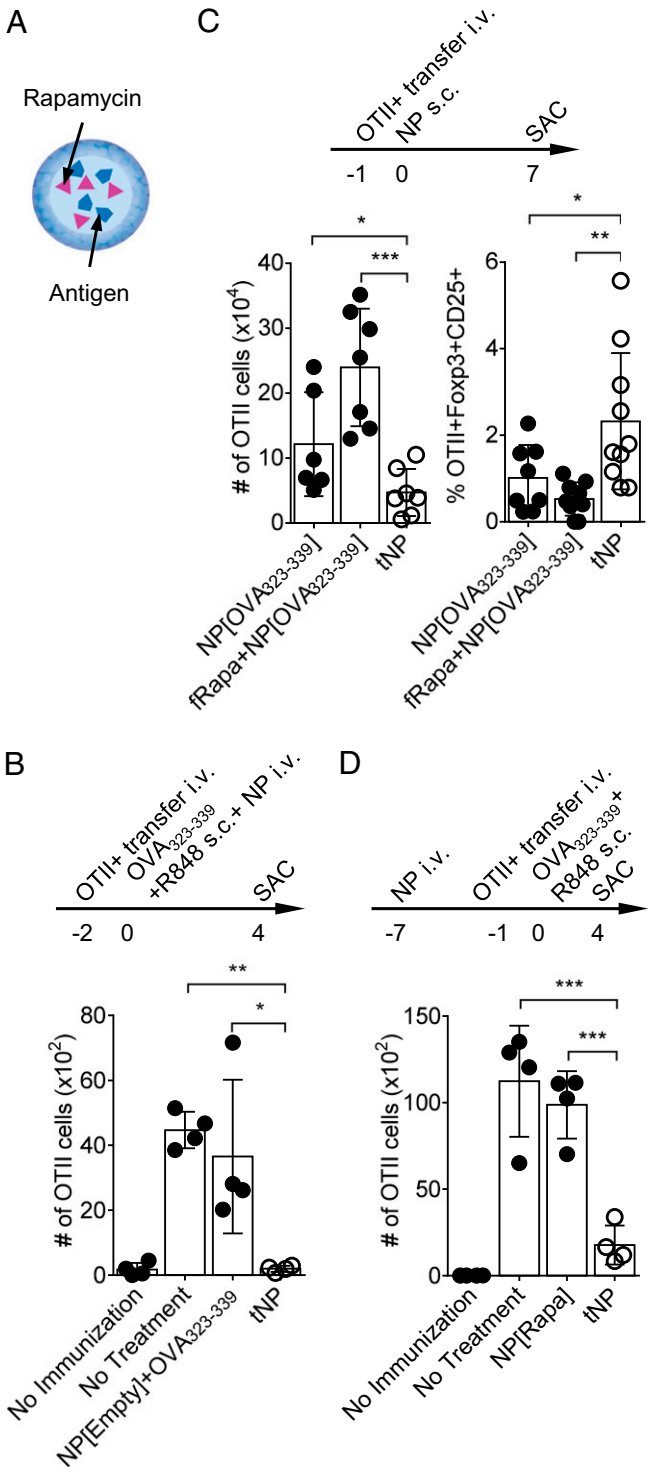

Fig. 1. tNPs in the CD4+ T-cell response. (*A*) tNP platform. Modular, synthetic, self-assembling tolerogenic PLGA NPs contain antigen and rapamycin. (*B*) NPs containing antigen and rapamycin (but not antigen alone) are tolerogenic. OTII T cells were transferred into CD45.1 mice on day −2. At day 0, animals received s.c. immunizations with vehicle (no immunization) or $OVA_{323–339}$ admixed with R848. At the same time, animals were injected i.v. with saline (no treatment), empty NPs admixed with $OVA_{323–339}$ (NP[Empty]+$OVA_{323–339}$), or tNPs (rapamycin+$OVA_{323–339}$). Four days later, popLNs were harvested and the total number of OTII T cells were quantified by flow cytometry (n = 4 per group). Data are representative of two independent experiments. (*C*) Encapsulation of rapamycin is critical for the control of CD4+ T-cell responses by tNP. OTII T cells were transferred into CD45.1+ mice 1 d before s.c. injection of tNPs (containing rapamycin and $OVA_{323–339}$) or NP[$OVA_{323–339}$] alone or NP[OVA323–339] admixed with free rapamycin (fRapa+NP[$OVA_{323–339}$]). Seven days later, popLNs were harvested, and total number of OTII cells was enumerated (*Left*) and the percentage of Foxp3+CD25+ OTII T cells was determined (*Right*). Data are cumulative of two independent experiments (n = 5). (*D*) Induction of antigen-specific MHC class II-restricted CD4 T-cell tolerance using tNP. C57BL/6 mice were treated i.v. on day −7 with NP[Rapa] or tNPs (rapamycin+$OVA_{323–339}$). On day −1, purified naïve CFSE-labeled CD4+OTII T cells were administered i.v., and then mice were immunized with $OVA_{323–339}$+R848 s.c. in the hind limbs on day 0. On day 4, popLNs were harvested and analyzed as in *B*. Data are representative of two independent experiments (n = 3 or 4 per group). All statistical analyses were performed using a one-way ANOVA with a Bonferroni posttest (***$P \leq 0.001$).

tolerance induced by tNP treatment, animals were given three biweekly doses of tNPs concurrently with OVA+CpG immunizations and then boosted 14 times with OVA in the absence of further tNP treatment (Fig. 3*B*). Anti-OVA titers in the tNP-treated animals did not become detectable until day 58 and remained ∼30–35-fold lower than that of untreated animals even in the absence of tNP treatment between days 42–234. Anti-OVA antibody titers remained well controlled in the tNP-treated animals even following challenge with OVA+CpG on days 239 and 253. Importantly, therapeutic administration of tNPs in mice with preexisting anti-OVA antibody titers attenuated further boosting with antigen even when the tNPs were coadministered with CpG (Fig. 3*C*).

Antigen-Specific Tolerance Induction by tNP Administration. Animals from Fig. 3*B* that had shown a long-lasting inhibition of anti-OVA responses were immunized and boosted with keyhole limpet hemocyanin (KLH). The tNP-treated mice showed a robust anti-KLH response (Fig. 4*A*) similar to that of the control animals, indicating they were not chronically immunosuppressed. To further test the specificity of the effect and show that the immunosuppressive effects of rapamycin are not broad or systemic, animals were injected s.c. with OVA+CpG ± tNP in the right limbs and KLH+CpG in the left limbs (Fig. 4*B*). Mixing tNP (containing $OVA_{323–339}$ and rapamycin) with OVA+CpG completely blocked the development of anti-OVA responses but had no effect on the anti-KLH response initiated in the contralateral limb (Fig. 4*B*). Moreover, a single injection of tNP containing OVA and rapamycin administered 14 d before repeated immunization with pOVA and KLH selectively inhibited the antibody response to OVA, but not KLH (Fig. 4*C*). In contrast, pretreatment at day −14 with control NP[Rapa] had no significant effect on the response to either OVA or KLH. In addition, animals that were treated three times every 2 wk with tNP+pOVA showed no detectable antibody response even at day 111 after five additional injections of pOVA in the absence of additional tNP treatment (Fig. 4*D*). Naïve animals in which pOVA immunizations were delayed until day 42 developed a robust anti-OVA response by day 84 after three injections of pOVA. These results further support the notion that tNP treatment did not lead to systemic immunosuppression and induced durable tolerance rather than merely delaying the immune response.

tNP Trafficking. To determine the fate of tNP after injection in vivo, cyanine 7 (Cy7) and Cy5 fluorescently labeled NPs were developed. Whole-body imaging by 3D fluorescence-based tomography (34) showed that fluorescent NPs rapidly and selectively accumulated in the liver and the spleen following i.v. administration (Fig. 4*E*, *Left* and Fig. S1 *A* and *B*). In contrast, fluorescent NPs administered s.c. in the hind limb showed rapid and selective accumulation in the draining LNs (Fig. 4*E*, *Right*). Immunohistochemical analysis of the spleen 24 h after i.v.

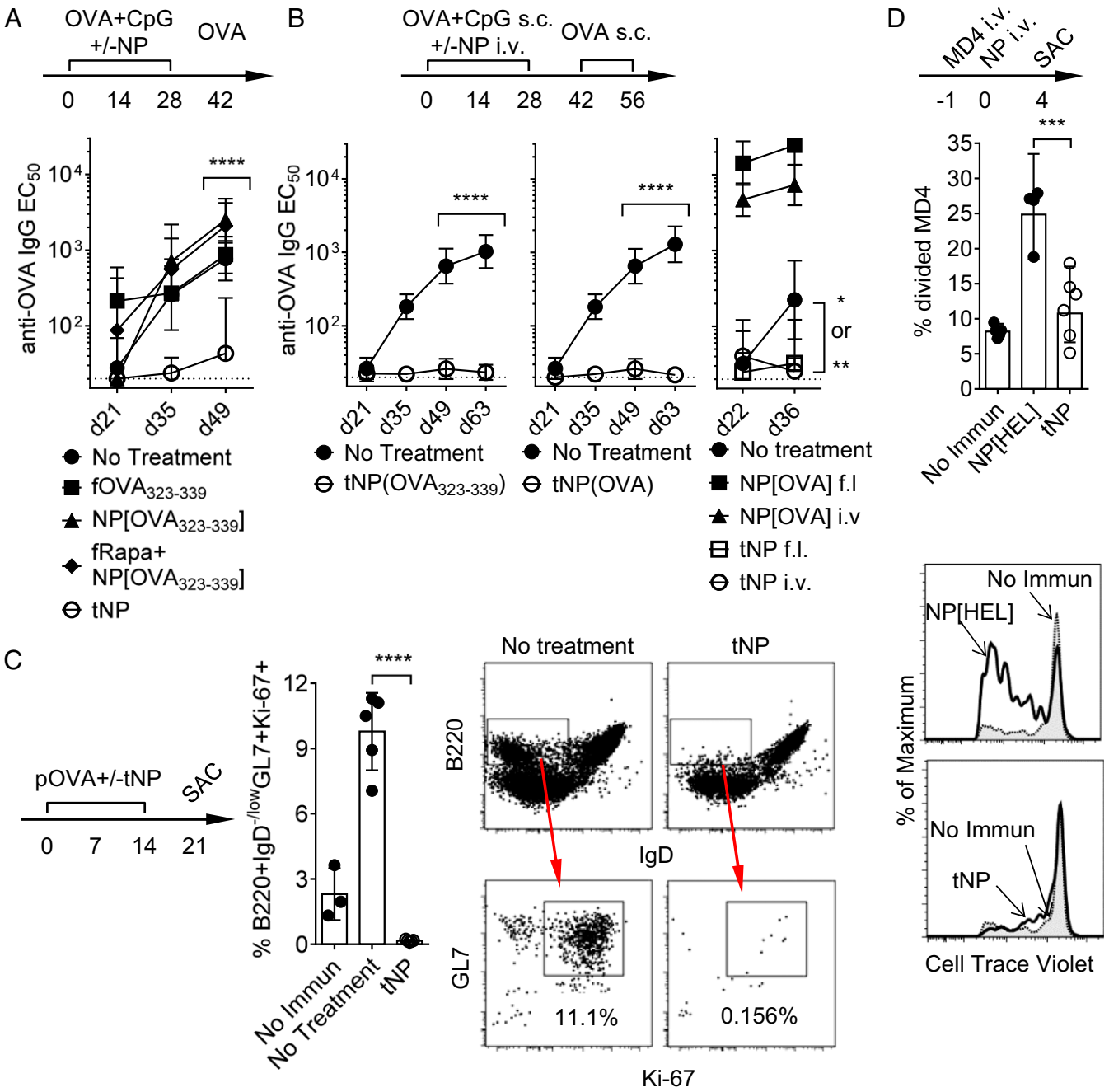

Fig. 2. tNPs in the humoral immune response. (*A*) Encapsulation of rapamycin is critical. C57BL/6 mice were injected s.c. on days 0, 14, and 28 with OVA+CpG together with vehicle (no treatment), tNP (rapamycin+$OVA_{323–339}$), free $OVA_{323–339}$ ($fOVA_{323–339}$), NP[$OVA_{323–339}$] alone, or NP[$OVA_{323–339}$] admixed with free rapamycin (fRapa+NP[$OVA_{323–339}$]). Animals were boosted with OVA on day 42, and anti-OVA IgG titers were determined by ELISA. Data are representative of four independent experiments (n = 3–5). (*B*) Both peptide and protein formulations of tNP are effective. C57BL/6 mice were immunized s.c. in the hind limbs on days 0, 14, and 28 with OVA+CpG and then boosted with OVA on days 42 and 56. In the *Left* and *Middle* panels, animals were treated on days 0, 14, and 28 with tNP containing rapamycin and either $OVA_{323–339}$ peptide or OVA protein, as indicated. Data are representative of three independent experiments (n = 5). In the *Right* panel, animals were treated s.c. in a distal site (front limb, f.l.) or i.v. with tNPs (OVA+rapamycin) or OVA-only NPs (NP[OVA]). The P values represent the difference between the tNP-treated groups and the no-treatment groups. (*C*) Prevention of germinal center B cells with tNP. C57BL/6 mice were injected i.v. with pOVA admixed with saline (no treatment) or tNP containing rapamycin and $OVA_{323–339}$ on days 0 and 14. On day 21, splenocytes were analyzed by flow cytometry for germinal center B cells (B220+CD19+TCRb– lymphocytes; n = 3, representative of two independent experiments). (*D*) Reduction of naïve B-cell activation with tNP. Cell trace violet-labeled MD4 B cells (5.10^6) were transferred i.v. into CD45.1+ animals. The next day mice were dosed i.v. with saline, HEL-only NPs (NP[HEL]), or tNPs (rapamycin+HEL). Four days later, spleens were analyzed for MD4 B-cell proliferation. The plots show the percentage of MD4 B cells that enter the cell cycle from the input (*Left*) and representative examples of the proliferation profile of each cell population (*Right*). The results summarize three independent experiments (n = 2–3). The symbols and bars in all figures represent the geometric mean ± 95% confidence interval. Statistics were performed using a one-way ANOVA with a Bonferroni posttest (****$P \leq 0.0001$).

injection of NP–Cy5 showed a typical distribution for a particulate antigen, colocalizing with the macrophages and DCs of the red pulp and the marginal zone that delimits the white pulp (Fig. 4*F*). FACS analysis confirmed that most myeloid cells, including

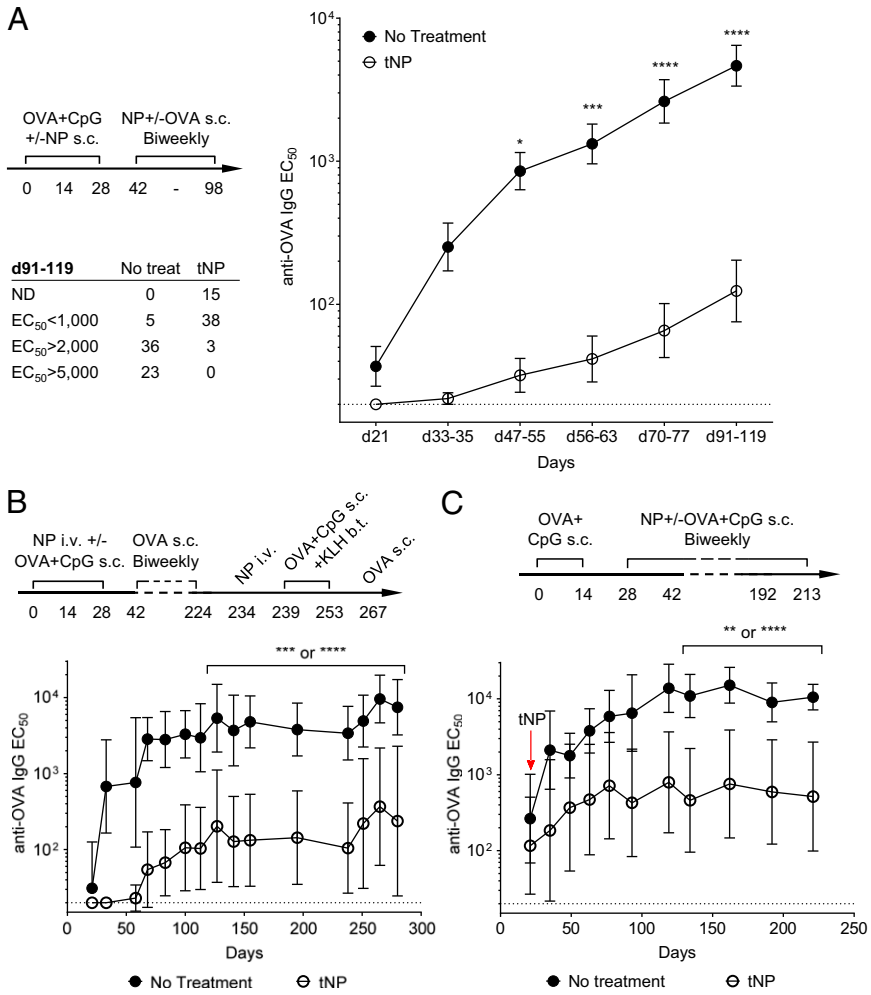

Fig. 3. Sustained and robust control of antibody responses with tNP. (*A*) Long-term effect of tNP. C57BL/6 animals were immunized s.c. with OVA+CpG on days 0, 14, and 28 and boosted with OVA every 14 days until at least day 77 with or without tNP (containing rapamycin+$OVA_{323–339}$). The figure depicts the anti-OVA IgG titers for the indicated range of days. Each dot represents the average titer for each group taken from nine independent experiments (n = 51 and 53 animals per group). The table shows the number of animals in each group with the indicated level of anti-OVA titers at the last bleed day (between day 91 and day 119). (*B*) Durability of tNP therapy. Mice were immunized s.c. with OVA+CpG and treated i.v. with vehicle (no treatment) or tNP (rapamycin+$OVA_{323–339}$) on days 0, 14, and 28. Animals were boosted with OVA every 14 d from day 42 to day 224 without any further tNP treatment. The treated group received another injection of tNP on day 234. The animals were subsequently challenged with OVA+CpG s.c. on days 239 and 253, followed by a boost of OVA s.c. on day 267 (n = 5). (*C*) Therapeutic tNP treatment inhibits further boosting of antigen titers. Animals were immunized s.c. with OVA+CpG on days 0 and 14 without any treatment. At day 21, anti-OVA titers were measurable in all animals. The untreated control group continued to receive injections of OVA+CpG every 2 wk from days 28–213, whereas the treated group received biweekly OVA+CpG supplemented with tNP (rapamycin+$OVA_{323–339}$) starting at day 21. EC_{50} was determined by ELISA (n = 5). The symbols represent the geometric mean ± 95% confidence interval. Statistics were performed using a two-way ANOVA with a Bonferroni posttest (****$P \leq 0.0001$).

macrophages, conventional DC (cDC), and plasmacytoid DC (pDC), contained particles (Fig. S1*C*) (16, 30, 31). These results show that our NPs efficiently deliver their payload to APCs in the lymphoid organs.

Effects of tNP in Animal Models of Hypersensitivity. Animals repeatedly immunized i.v. with pOVA developed anaphylactoid responses after three weekly i.v. infusions of pOVA, reminiscent of the antibody-mediated hypersensitivity reactions observed in some patients who develop antidrug antibodies (35–37). Untreated animals with high titers against OVA from Fig. 4*C* exhibited strong hypersensitivity to pOVA administered i.v., whereas animals that received a single prophylactic treatment of tNP showed no anti-OVA titers and were largely protected from anaphylaxis (Fig. 5*A*). Similarly, animals immunized with OVA+CpG and challenged with OVA s.c. experienced a significant delayed-type hypersensitivity (DTH) response on the day after challenge, whereas animals that received concomitant tNP treatment during immunization showed no inflammation (Fig. 5*B*). In addition, prophylactic treatment with tNP (containing OVA+rapamycin) administered 4 d before immunization to induce an anti-OVA CD8 T-cell response inhibited the subsequent in vivo killing of labeled target cells loaded with $OVA_{257–264}$ (SIINFEKL), an MHC class I-restricted peptide of OVA (Fig. 5*C*). Next, the efficacy of tNP was tested in animals with allergic disorders. Animals treated with tNP during oral (Fig. 5*D*) or i.p. sensitization (Fig. 5*H*) showed complete inhibition of both anti-OVA IgG and IgE antibody responses. Immunization with OVA and aluminum hydroxide gel (Alum) i.p. followed by intragastric (i.g.) or intranasal (i.n.) challenge with OVA induced the development of oral allergy or allergic airway inflammation, respectively. Sensitized animals treated therapeutically with tNP i.v. at the time of oral challenge showed a reduction in anaphylaxis (sickness score, diarrhea, and temperature drop; Fig. 5*E*). Serum levels of mouse mast cell protease 1 (mMCP1) in recently challenged animals were also reduced by prior treatment with tNP (Fig. 5*F*). No effect was observed on the levels of serum anti-OVA IgE concentration using this therapeutic protocol. In animals with allergic airway inflammation induced by challenge with OVA i.n. (Fig. 5*G*), therapeutic tNP treatment after establishment of the allergic reaction reduced the number of lymphocytes (CD8+ and CD4+ T cells and B cells) and eosinophils in the bronchoalveolar lavage (BAL) fluid. Treatment with tNPs also resulted in decreased numbers of splenic T cells with an activated phenotype (CXCR5+TCRβ+CD19–CD45R–) and an increased proportion of cells with a B regulatory phenotype (CD19+CD45R+IL-10+) compared with saline-treated animals. Similar to animals with oral allergies, no significant effect was observed on the IgE levels using this therapeutic protocol (Fig. 5*G*). However, concurrent treatment with tNP during immunization (days, 0, 7, and 14) suppressed the IgE response and completely blocked the recruitment of lymphocytes to the airways in the presence of OVA (Fig. 5*H*). Importantly, no adverse events were observed even when tNPs were administered i.v. to animals with high serum levels of antigen-specific IgG and/or IgE. Together these results show that

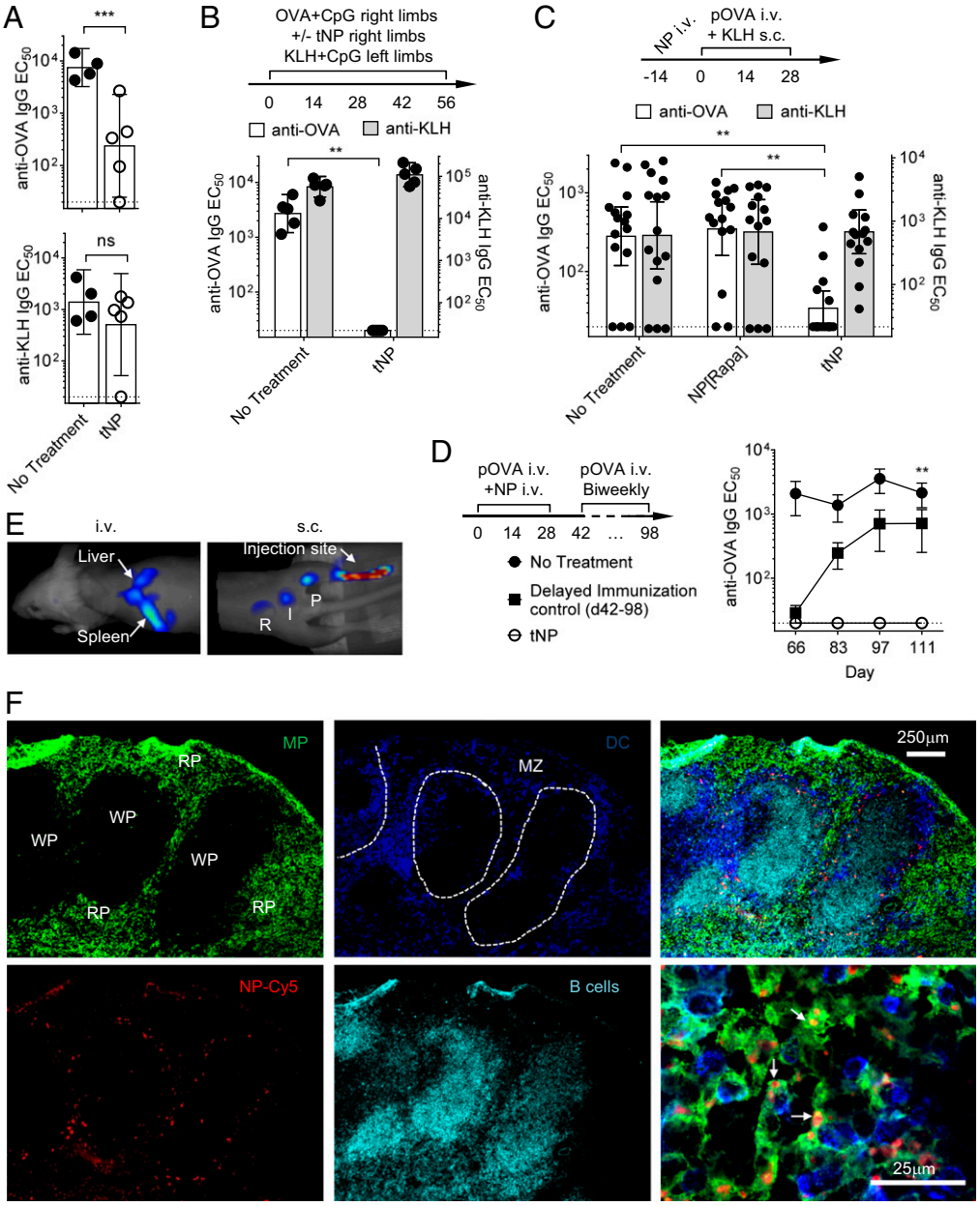

Fig. 4. Antigen specificity of tolerance induction by tNP. (*A*) Antigen specificity of tNP therapy. Animals from Fig. 3*B* were immunized s.c. with 50 μg of KLH on both lateral flanks at the base of the tail (b.t.) on days 239, 253, and 267. Anti-KLH IgG and anti-OVA IgG titers from each animal on day 280 are shown. (*B*) Treatment with tNP does not result in broad immunosuppression. C57BL/6 mice were immunized with OVA+CpG in the right (front and hind) limbs and with KLH +CpG in the left limbs, whereas treated animals received OVA+CpG+tNP injections in the right limbs and KLH+CpG in the left limbs every 2 wk for 8 wk. Anti-OVA and anti-KLH titers were determined by ELISA ($n = 5$). (*C*) Prophylactic induction of antigen-specific tolerance. C57BL/6 mice were treated with a single injection i.v. of tNPs (rapamycin+OVA), NP[Rapa], or vehicle (no treatment) on day −14. Mice were immunized with pOVA i.v. and KLH s.c. on days 0, 14, and 28. Anti-OVA and anti-KLH titers were assessed on day 41. The results summarize three independent experiments ($n = 5$). (*D*) Durability of prophylactic induction of antigen-specific tolerance. Two groups of C57BL/6 animals (no treatment and tNP-treated) were immunized biweekly with eight injections with pOVA i.v. from day 0 to day 98. The treated group received tNP (rapamycin+OVA) for the first three immunizations only (days 0, 14, and 28). The start of immunization for a third group of animals was delayed until day 42 (delayed immunization control). In all figures and panels, the bars and the symbols represent the geometric mean ± 95% confidence interval ($n = 5$). All *P* values were calculated using a Bonferroni posttest of a regular one-way or two-way ANOVA test (***$P \leq 0.001$). (*E*) In vivo trafficking of tNP. (*Left*) (i.v. injection) Balb/C animals were immunized with pOVA on days −27 and −13. On day 0, fluorescently tagged Cy7–tNP containing OVA and rapamycin were injected i.v., and the animals were imaged by 3D FMT at 6 h after injection. (*Right*) (s.c. injection) Naïve Balb/C mice were injected with fluorescently tagged Cy7–tNP s.c. and then imaged 1 h after injection ($n = 3$). I, iliac; *P* = popLNs; R, renal. (*F*) Cellular localization of tNP. Fluorescently tagged NP–Cy5 (red) NPs were injected i.v., and spleens were harvested 24 h later for cryosectioning and immunohistochemical analysis. Shown are representative low and high (*Lower Right* panel) magnification (10× and 100×, respectively) photomicrographs of the distribution of the NPs among the red pulp (RP), the white pulp (WP), and the marginal zone (MZ) delineated by the localization of macrophages (MPs, F4/80, green), DCs (CD11c, dark blue), and B cells (B220, cyan).

treatments with tNP during or after sensitization are safe and can significantly reduce inflammatory processes associated with hypersensitivity reactions.

Prophylactic and Therapeutic Efficacy of tNP in a Relapsing–Remitting Model of Experimental Autoimmune Encephalomyelitis. Empty NP or tNP containing rapamycin and $PLP_{139–151}$ were administered

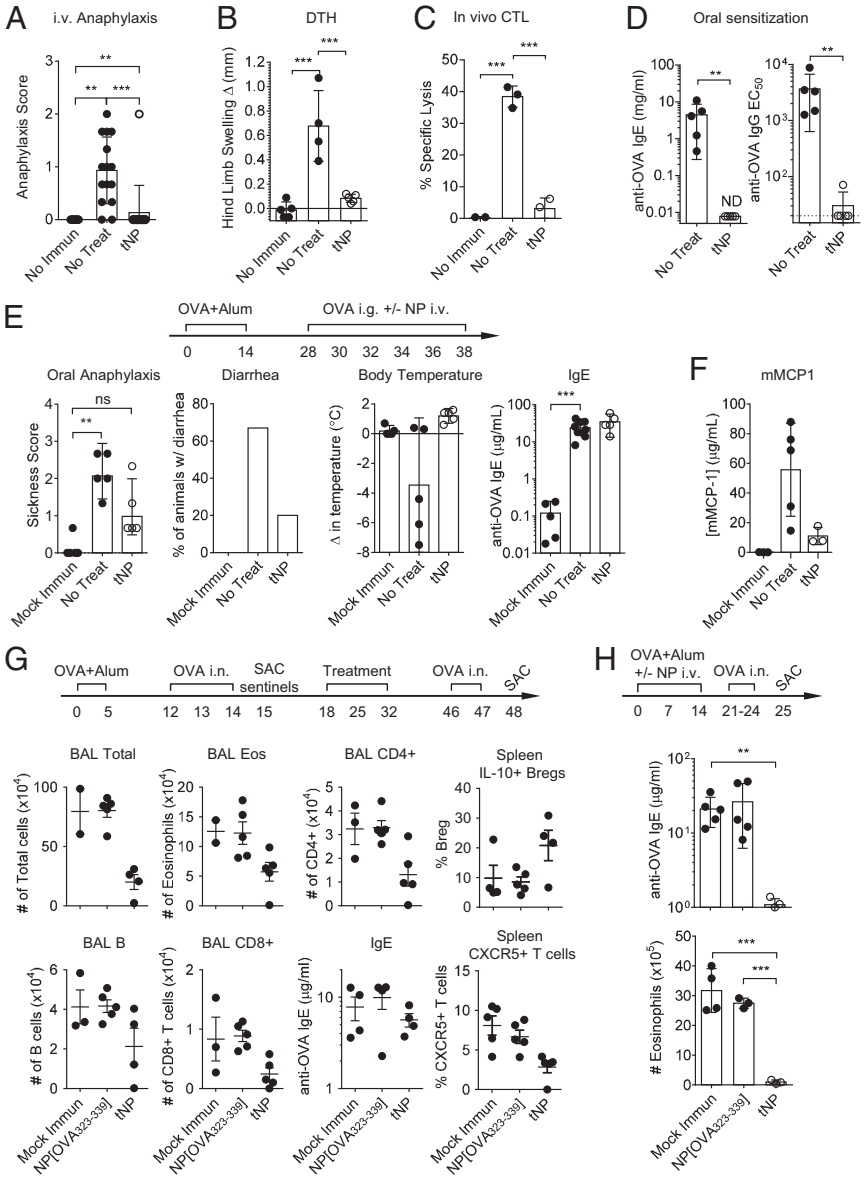

Fig. 5. Prevention and amelioration of hypersensitivity disorders by tNP. (*A*) Inhibition of anaphylactic response to i.v. antigen. Anaphylactic reactions in response to the third i.v. injection of pOVA in animals described in Fig. 4*C* were assessed by three blinded scorers (0, no symptom; 1, lethargy; 2, lethargy and inability to right; 3, moribund). The results summarize three independent experiments ($n = 5$). (*B*) Inhibition of anti-OVA DTH response. C57BL/6 mice were immunized s.c. with OVA+CpG in the front limbs and treated i.v. with tNP or saline on days 0, 14, and 28. Animals were challenged s.c. on day 34 with 25 μg of OVA in one hind paw and saline in the other. The next day the difference in thickness between the two limbs was determined using a caliper. Data are representative of two independent experiments ($n = 5$). (*C*) In vivo cytotoxic T-lymphocyte (CTL) assay. Animals were treated with tNP or PBS on days 0 and 5 and then immunized with NP-encapsulated OVA and CpG on day 9. On day 14, animals received a mixture of CFSE-labeled target cells loaded with the MHC class I-restricted OVA peptide $OVA_{257-264}$ SIINFEKL and labeled control cells. The next day, spleens were harvested and specific lysis of target cells was determined by flow cytometry ($n = 3$). (*D*) Inhibition of orally induced IgG and IgE responses using tNP. BALB/c mice were sensitized i.g. with OVA (5 mg) and cholera toxin (CTx, 10 μg) weekly for 10 wk. Mice were treated i.v. with saline (no treatment) or tNP (rapamycin+OVA). Anti-OVA titers were assessed on day 83 ($n = 5$). (*E*) Inhibition of anaphylactic response to an oral allergen. Balb/C mice were immunized with OVA+Alum on days 0 and 14 and challenged six times with OVA by i.g. gavage every 2 d from day 28 until day 38. Animals were treated i.v. with saline (no treatment) or tNP (rapamycin+OVA) during each oral challenge. Mock immunized animals received Alum. Animals were assessed by three blinded scorers for anaphylaxis, and the percent of animals with diarrhea. The changes in body temperature were also recorded. Anti-OVA IgE was assessed on day 38. Data are representative of two independent experiments ($n = 5$). (*F*) Inhibition of mMCP1 release. Balb/C animals were immunized with OVA+Alum and then challenged orally with OVA while receiving treatment with tNPs. Serum mMCP1 levels were assessed 1 h after the last (sixth) challenge by ELISA ($n = 5$). (*G*) Effect of therapeutic treatment with tNP on allergic airway inflammation. Balb/C animals were injected with OVA+Alum on days 0 and 5 and then challenged with OVA i.n. on days 12, 13, and 14. A sentinel group of animals killed on day 15 were confirmed to have allergic airways. At days 18, 25, and 32, animals received i.v. treatments of saline, NP[$OVA_{323-339}$], or tNPs (rapamycin+$OVA_{323-339}$). BAL fluid was collected after challenge and assessed for T cells, B cells, and eosinophils. Splenocytes were restimulated overnight with OVA and assessed for TCRβ+CXCR5+ T cells and CD19+B220+IL-10+ cells (Bregs). (*H*) Inhibition of IgE responses and airway reactivity using tNP. BALB/c animals were injected with OVA+Alum on days 0, 7, and 14 and then challenged daily with OVA i.n. from day 21–24. Animals were treated i.v. with saline (no treatment), NP[$OVA_{323-339}$], or tNP (rapamycin+$OVA_{323-339}$) on days 0, 7, and 14. The results are representative of two independent experiments ($n = 5$). The bars in all figures and panels represent the geometric mean (±95% confidence interval). All *P* values were calculated using a Bonferroni posttest of a regular one-way or two-way ANOVA test (***$P \leq 0.001$).

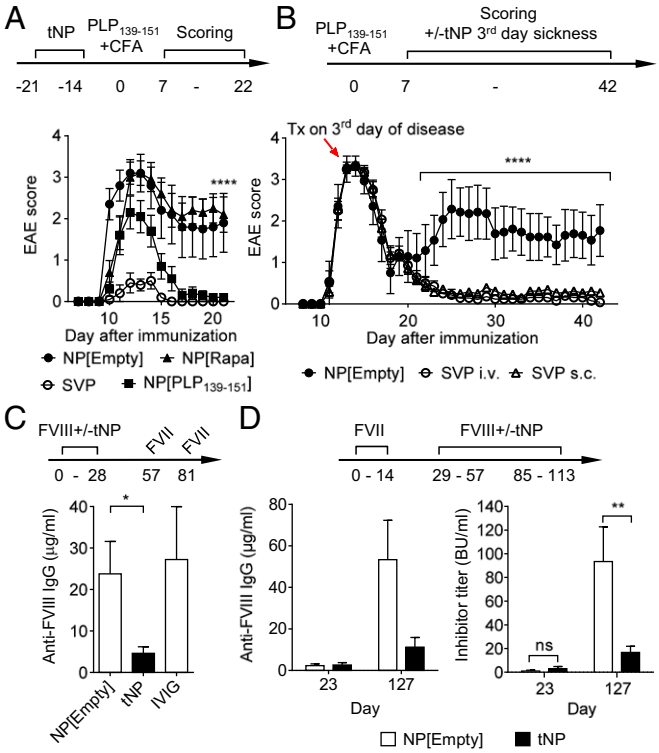

Fig. 6. Induction of tolerance in R-EAE and hemophilia A mice using tNP. (*A*) Prophylactic treatment of EAE. SJL mice (n = 12) were treated prophylactically i.v. with tNP ($PLP_{139–151}$ and rapamycin) or placebo NPs (NP [Empty]) on day −21 and −14. R-EAE was induced by injecting $PLP_{139–151}$+CFA and pertussis toxin (PTx) on day 0. EAE disease symptoms were scored by blinded observers. (*B*) Therapeutic treatment of EAE. EAE was induced in SJL mice (n = 13–14 per group) by injecting $PLP_{139–151}$/CFA. Animals were individually monitored for onset of disease and treated therapeutically on the third day of detectable disease (around day 13) with either empty NP or tNP. Results are represented as the mean ± 95% confidence interval. For statistical analysis, Student t test with two-tailed distribution was used (****P < 0.0001). (*C*) Inhibition of anti-FVIII responses in naïve hemophilia A mice. FVIII KO hemophilia A mice (E16, n = 8 at day 0) received five weekly i.v. injections of rhFVIII together with tNP (rapamycin+FVIII peptides), empty NPs, or IVIG. The mice were then challenged with 1 µg of FVIII on days 57 and 81 without treatment. Anti-FVIII antibody levels (day 95) were determined by ELISA. (*D*) Therapeutic efficacy of tNP treatment on anti-FVIII and inhibitor titers in E16 mice. Hemophilia A mice received three weekly i.v. injections of rhFVIII. Anti-FVIII antibody levels were determined on day 23, and primed E16 mice were then assigned into two groups. Starting on day 29, one group of the mice received two rounds of five weekly i.v. injections of rFVIII+tNP (rapamycin+FVIII peptides). The control group received rhFVIII+NP[Empty]. The data show the anti-FVIII antibody levels 2 wk after the last therapeutic injection (day 127). Anti-FVIII titers were quantified using a standard curve generated with a mixture of monoclonal anti-FVIII A2 and C2 antibodies, whereas FVIII inhibitor titers (BU/mL) were determined using a modified Bethesda assay. Data are expressed as mean ± SEM. For statistical analysis, Student t test with two-tailed distribution was used (**P < 0.01).

prophylactically to SJL mice by s.c. injection 21 and 14 d before immunization with $PLP_{139–151}$/CFA to induce relapsing–remitting experimental autoimmune encephalomyelitis (R-EAE). Treatment with tNP inhibited the onset and severity of paralysis typical of this model of autoimmunity (Fig. 6*A* and Fig. S2*A*) and inhibited weight loss (Fig. S2). The animals were followed for 3 wk to exclude the possibility of a delayed response. Mice treated with NP[Rapa] showed only a modest delay in disease onset, whereas animals treated with NP containing only the $PLP_{139–151}$ peptide showed partial protection. Importantly, animals treated therapeutically with a single i.v. injection of tNP administered near the peak of disease showed complete inhibition of disease relapse (Fig. 6*B* and Fig. S2*B*). Therapeutic treatment with tNP by s.c. injection resulted in complete inhibition of relapse in 12 of 13 mice (Fig. 6*B*).

Induction of Tolerance to FVIII in Hemophilia A Mice. Hemophilia A mice deficient in the expression of FVIII (E16) present with similar defects in blood clotting and propensity to develop neutralizing antibodies against recombinant human FVIII (rhFVIII) as severe hemophilia A patients. Administration of rhFVIII led to the development of neutralizing antibody responses or "inhibitors" that block the procoagulant function of the therapeutic rhFVIII, similar to previous studies (38). Prophylactic administration of tNPs given at the same time as rhFVIII administration in naïve mice (Fig. 6*C*) or therapeutic administration of tNPs in mice previously primed with three injections of rhFVIII led to a significant reduction of anti-FVIII antibodies, including neutralizing antibodies (Fig. 6*D*).

Discussion

We were guided by the following design criteria in developing tNPs: (*i*) use of a polymer (PLGA) that is biocompatible, biodegradable, and used in multiple products licensed for clinical use by regulatory agencies, (*ii*) a small-molecule immunomodulatory agent (rapamycin) that has been validated in humans and is capable of securing immune tolerance programming even in the face of inflammatory signals, (*iii*) nano-sized particles to allow for efficient transport to lymphoid organs and capture by APCs, and (*iv*) concomitant delivery of either protein or peptide antigens with the small-molecule immunomodulator, thus enabling coordinated delivery of immunological instructions to APCs. Importantly, we have previously validated the manufacturing process for PLGA NPs through the successful production of multiple GMP lots that were released and used in a phase 1 vaccine clinical trial (39).

We show here that the tNPs are capable of inducing antigen-specific B-cell tolerance that is maintained for at least 200 d in the face of repeated challenges with antigen (Fig. 3*B*). Treatment with tNPs through a variety of routes (i.v. and s.c.) and schedules of treatment efficiently inhibited B-cell activation and antibody responses against antigens administered locally or systemically (i.v., s.c., i.g., and i.p.; Figs. 2 *B*–*D*, 4*C*, and 5) as well as local and systemic hypersensitivity reactions (Fig. 5 *A*, *B*, and *E*). Importantly, tNPs were capable of inducing tolerance even when coadministered with free antigen in the presence of potent TLR agonists, such as CpG or R848, and adjuvants, such as Alum and CTx (Figs. 1*B*, 3 *A* and *B*, and 5). Prophylactic administration of tNPs inhibited anti-OVA IgE antibody production in allergy models (Fig. 5 *D* and *H*). Therapeutic treatment had no effect on anti-IgE levels but attenuated the pathological effects of antigen administration in a model of oral allergy (Fig. 5*E*) and allergic airway inflammation (Fig. 5*G*). These results suggest that the beneficial effects mediated by tNP treatment after immunization could be exerted on the cellular compartment responding to the antigen rather than on the antibody levels per se. It is possible that therapeutic reduction of preexisting antibody levels would require more time due to the presence of long-lived plasma cells. However, therapeutic administration of tNPs applied on preexisting anti-OVA IgG responses and inhibited further boosting with the antigen even in the presence of CpG (Fig. 3*C*), suggesting an inhibitory effect on the memory cells responsible for the secondary or boost response. We believe that there are both temporal and spatial aspects to the induction of antigen-specific immune tolerance with tNPs. The temporal aspect of tolerance induction is illustrated in Fig. 4*C*, where tNPs are administered 14 d before repeated immunization with OVA and KLH. In this experiment, the tNP containing OVA and rapamycin selectively inhibits the antibody response to OVA but not KLH, whereas

NPs containing only rapamycin have no effect on either response. In contrast, Fig. 4*B* illustrates the spatial aspect of antigen-specific tolerance induction, where tNP and OVA+CpG are administered in the left flank and KLH+CpG is administered at the same time in the right flank. Because the tNP biodistribution following s.c. administration is localized to the draining LNs (Fig. 4*E*, *Right*), the tNP selectively inhibits the immune reaction against OVA in the LNs, draining the left flank without affecting the immune response to KLH in the right flank.

The precise mechanism of action of our tNPs remains to be determined. Nanoparticulates have been shown to be selectively endocytosed by APCs, such as macrophages and DCs (16, 30, 31). The codelivery of antigen and rapamycin provide an instruction set that could allow for the conditioning of tolerogenic DCs capable of inducing CD4+ Treg (22, 23). In support of this notion, prophylactic treatment with $OVA_{323–339}$–loaded tNPs 7 d before transfer of OTII T cells resulted in complete inhibition of OTII T-cell expansion in response to immunization with $OVA_{323–339}$+R848, whereas treatment with control NPs containing only rapamycin had no effect (Fig. 1*D*). These experiments show that the inhibitory effect induced by the tNPs is more durable than that expected from transient immunosuppression by rapamycin and is dependent on the presence of antigen, indicating the formation of $OVA_{323–339}$–specific regulatory cells that can control the activation of the subsequently transferred OTII T cells. Indeed, tNP treatment induced an increase in the percentage of FoxP3+ antigen-specific T cells (Fig. 1*B*). Importantly, we found that admixing free rapamycin with NP-encapsulated OVA (or $OVA_{323–339}$) did not result in immune tolerance. In fact, free rapamycin, administered at an equivalent dose as that used in tNP treatment, showed the opposite trend with respect to inhibition of OVA-specific T-cell expansion and induction of antigen-specific Tregs, perhaps due to the direct effect of free rapamycin on enhancing effector memory T-cell formation (40). Moreover, free rapamycin showed a consistent trend toward enhancing anti-OVA–specific antibody responses. Similarly, NPs loaded with protein antigen in the absence of rapamycin were very immunogenic. These results indicate that the biology of both the rapamycin and the antigen can be profoundly influenced by the context in which they are delivered.

Tolerance induction using NPs was also demonstrated by Yeste et al. (19), using gold NPs loaded with 2-(1′H-indole-3′-carbonyl)-thiazole-4-carboxylic acid methyl ester (or ITE, a ligand for the aryl hydrocarbon receptor) and $MOG_{35–55}$ (MHC class II-restricted peptide from myelin oligodendrocyte glycoprotein) in a model of EAE. In contrast, Getts et al. (13) demonstrated tolerogenic activity of $PLP_{139–151}$ conjugated to polystyrene or PLGA microparticles in the absence of any immunomodulator. Induction of tolerance with NPs containing only antigen was not observed by us (Fig. 2*B*) or by Yeste et al. (19). However, the larger, highly negatively charged particles used by Getts et al. (13) may induce tolerance through an alternative mechanism via MARCO+ macrophages.

One of the potential risks of antigen-based immunotherapy is that administration during an ongoing inflammatory event could potentially override tolerogenic programming, resulting in disease exacerbation. This is a phenomenon well known in allergy immunotherapy in which administration of the antigen can result in adverse events, including anaphylaxis (41). We have attempted to mitigate this risk by using an immunomodulatory agent, rapamycin, which can induce and maintain the tolerogenic programming, even in the presence of potent TLR agonists. Another potential advantage of our tNPs is the ability to incorporate whole protein antigen, which is an important consideration for clinical application in a heterogeneous human population, particularly for large complex proteins, like FVIII, that contain many MHC class II epitopes. NPs containing protein antigen without rapamycin are immunogenic (Fig. 2 *B* and *D*), whereas the encapsulation of rapamycin in the NPs, but not admixed free rapamycin, induces tolerance. To our knowledge, the only other NPs capable of presenting and inducing tolerance to whole protein antigens are the liposomes bearing the CD22 ligand described by Macauley et al. (18), which induce B-cell, but not T-cell, tolerance. Finally, it is notable that our tNPs are capable of inhibiting immune responses when administered either i.v. or s.c., whereas other NP approaches appear to be limited to systemic administration (13, 19, 32). More experimentation is necessary to compare these technologies and determine whether they can be used in similar applications.

The emergence of NP-based therapies for the induction of antigen-specific immune tolerance holds considerable promise for the future of immunotherapy. Tolerogenic therapies could be beneficial for the treatment of allergic asthma, life-threatening food allergies, and autoimmune disease (8). A single therapeutic dose of tNP administered at the peak of disease completely inhibited disease relapse in EAE, a model of human multiple sclerosis (Fig. 6*B*). Antigen-specific tolerance could be useful in preventing antidrug antibodies, which can compromise efficacy and safety of biologics. A prominent example is the neutralizing antibody responses to FVIII, which results in major complications for up to 30% of hemophilia A patients (42). Currently patients that develop inhibitors are treated with large and frequent doses of FVIII, which is extremely costly. Here we show that adding tNP to the therapeutic regimen of FVIII for a limited number of injections allows for the establishment of tolerance (Fig. 6 *C* and *D*). Protein therapies are the fastest growing segment of new drug approvals, and a proliferation of novel engineered proteins, such as multivalent antibodies and antibody-drug conjugates, may be at increased risk for immunogenicity (43). tNPs could potentially also be applied to prevent immunogenicity associated with vectors used for gene therapy. The ability to translate antigen-specific therapy to human clinical practice would represent a breakthrough that could potentially benefit patients across a wide spectrum of clinical indications.

Materials and Methods

Complete details of materials are provided in *SI Materials and Methods*.

tNP and NP Manufacturing. tNPs containing both antigen and rapamycin were prepared using a water-in-oil-in-water double emulsion solvent evaporation method (44, 45). Briefly, PLGA, pegylated polylactic acid (PLA-PEG), and rapamycin were dissolved in dichloromethane to form the oil phase. An aqueous solution of antigen (OVA protein, $OVA_{323–339}$ peptide, $FVIII_{75–89}$ peptide, $FVIII_{1723–1737}$ peptide, $FVIII_{2191–2210}$ peptide, or $PLP_{139–151}$ peptide) was then added to the oil phase and emulsified by sonication (Branson Digital Sonifier 250A). Following emulsification of the antigen solution into the oil phase, a double emulsion was created by adding an aqueous solution of polyvinylalcohol and sonicating a second time. The double emulsion was added to a beaker containing phosphate buffer solution and stirred at room temperature for 2 h to allow the dichloromethane to evaporate. When creating NPs containing rapamycin but no antigen, or NPs without any encapsulated agents, a similar oil-in-water single emulsion process was used. The resulting NPs were washed twice by centrifuging at 75,600 × *g* and 4 °C followed by resuspension of the pellet in PBS. Fluorescent Cy5- and Cy7-containing NPs were manufactured as described above using PLGA–Cy5 or PLGA–Cy7 conjugate, respectively. PLGA with a butyl amine end group was prepared from PLGA–acid, which was then treated with Cy7–acid or Cy5–acid in the presence of a coupling agent (O-(Benzotriazol-1-yl)-N,N,N′,N′-tetramethyluronium tetrafluoroborate) to afford the conjugates.

Animal Models. Animal procedures involving hemophilia A mice, EAE, and in vivo imaging were approved by the Institutional Animal Care and Use Committee of the Uniformed Services University of the Health Sciences, Hooke Laboratories, and Molecular Research Imaging, respectively. All other mouse experiments were approved by the Institutional Animal Care and Use Committee of Avastus Preclinical Services, following local and national guidelines and regulations.

Relapsing EAE model. EAE was induced by injection of SJL mice s.c. at four sites in the back with $PLP_{139–151}$ emulsified in CFA (Hooke Laboratories) followed 2 h later by i.p. injection of 154 ng of pertussis toxin. Blinded EAE scores

were assessed daily starting from day 7, and body weight was measured three times per week. EAE was scored on a 0–5 scale as follows: 0, no obvious changes in motor functions of the mouse in comparison with nonimmunized mice; 1, limp tail; 2, limp tail and weakness of hind legs; 3, limp tail and complete paralysis of hind legs (most common) or limp tail with paralysis of one front and one hind leg; 4, complete hind leg and partial front leg paralysis; 5, death or euthanized because of severe paralysis.

Allergic airway model. BALB/c female mice aged 8–10 wk were sensitized by i.p. injections of 10 μg Ova adsorbed to 4 mg of Alum on days 0 and 5. On days 7, 8, and 9, mice were administered 25 μg Ova i.n. Mice were treated with tNP or PBS on days 25, 32, and 39. Finally, mice were administered PBS for the control group or 25 μg OVA i.n. for 3 consecutive days from days 46–48 and were killed 1 h after the last challenge by a lethal dose of isofluorane. Lungs were lavaged three times with 1 mL of ice-cold PBS containing 3 mM EDTA.

Oral allergy model. BALB/c female mice were sensitized by i.p. injections of 500 μg OVA adsorbed to 4 mg of Alum on day 0 and then 50 μg OVA adsorbed to 4 mg of Alum on day 14. On days 27, 29, 31, 34, and 36, mice were treated i.v. with tNP or PBS and challenged with 50 mg of OVA by i.g. gavage. Mice were evaluated for sickness by three blinded scorers as previously described (46, 47). Rectal temperatures and liquid stool scores were measured (0, dry; 1, wet) 1 h after the final challenge.

In vivo CTL assay. Test animals were immunized with NPs containing OVA protein and CpG oligodeoxynucleotides (ODN). Five days later, spleen cells harvested from naïve animals were loaded with low levels of carboxyfluorescein diacetate succinimidyl diester (CFSE) and the $OVA_{257–264}$ MHC class I-restricted peptide of OVA ($CFSE^{low}$, $SIINFEKL^{+}$ Targets), whereas another portion of cells were loaded with high levels of CFSE alone ($CFSE^{high}$, $SIINFEKL^{-}$ Control). A 1:1 mixture of these labeled target cells was injected into the recipient naïve and test animals to monitor specific killing of SIINFEKL peptide-presenting cells ($CFSE^{low}$) relative to their control ($CFSE^{high}$).

In Vivo FMT Imaging. In vivo 3D fluorescence tomography (FMT) imaging was performed by Molecular Imaging on the Perkin-Elmer FMT 2500 LX Quantitative Tomography Imaging System. Mice were injected with Cy7-labeled NPs and anesthesitized with 2% (vol/vol) isoflurane gas just before imaging. A scanning region was manually positioned over the body from the head to chest for scan 1 and from chest to hind limbs for scan 2. Each animal was scanned in that specific region of interest using a medium (3 mm) source density. Images were reconstructed and analyzed using Perkin-Elmer True Quant software.

Fluorescence Imaging. Frozen sections were fixed with cold acetone and stained for the indicated markers and visualized at room temperature using an upright epifluorescence microscope Leica DMI6000B system equipped with a Leica DFC340FX. Images were processed using ImageJ software.

ACKNOWLEDGMENTS. The authors gratefully acknowledge the excellent support of Aditi Chalishazar, Dr. Lynelle Pittet, and the ELISA team for ELISA analyses and Dr. Fen-ni Fu, Dr. William Kuhlman, Dr. Victor Chan, Ray Damien, and Dr. Nelly Viseux for analytical characterization of nanoparticles. We thank Dr. Suzana Marusic for support with the EAE studies. This work was partially funded by a grant from the Juvenile Diabetes Research Foundation.

1. Burks AW, et al. (2013) Update on allergy immunotherapy: American Academy of Allergy, Asthma & Immunology/European Academy of Allergy and Clinical Immunology/PRACTALL consensus report. *J Allergy Clin Immunol* 131(5):1288–1296, e1283.
2. Hayter SM, Cook MC (2012) Updated assessment of the prevalence, spectrum and case definition of autoimmune disease. *Autoimmun Rev* 11(10):754–765.
3. Nechansky A, Kircheis R (2010) Immunogenicity of therapeutics: A matter of efficacy and safety. *Expert opin drug discov* 5(11):1067–1079.
4. Zhang AH, Skupsky J, Scott DW (2009) Factor VIII inhibitors: Risk factors and methods for prevention and immune modulation. *Clin Rev Allergy Immunol* 37(2):114–124.
5. Banugaria SG, Patel TT, Kishnani PS (2012) Immune modulation in Pompe disease treated with enzyme replacement therapy. *Expert Rev Clin Immunol* 8(6):497–499.
6. Carbone J, del Pozo N, Gallego A, Sarmiento E (2011) Immunological risk factors for infection after immunosuppressive and biologic therapies. *Expert Rev Anti Infect Ther* 9(4):405–413.
7. Riminton DS, Hartung HP, Reddel SW (2011) Managing the risks of immunosuppression. *Curr Opin Neurol* 24(3):217–223.
8. Bluestone JA, Bour-Jordan H (2012) Current and future immunomodulation strategies to restore tolerance in autoimmune diseases. *Cold Spring Harb Perspect Biol* 4(11):pii: a007542.
9. Smarr CB, Hsu CL, Byrne AJ, Miller SD, Bryce PJ (2011) Antigen-fixed leukocytes tolerize Th2 responses in mouse models of allergy. *J Immunol* 187(10):5090–5098.
10. Miller SD, Wetzig RP, Claman HN (1979) The induction of cell-mediated immunity and tolerance with protein antigens coupled to syngeneic lymphoid cells. *J Exp Med* 149(3):758–773.
11. Scott DW, Long CA (1976) Role of self-carriers in the immune response and tolerance. I. B-cell unresponsiveness and cytotoxic T-cell immunity induced by haptenated syngeneic lymphoid cells. *J Exp Med* 144(5):1369–1374.
12. Battisto JR, Bloom BR (1966) Dual immunological unresponsiveness induced by cell membrane coupled hapten or antigen. *Nature* 212(5058):156–157.
13. Getts DR, et al. (2012) Microparticles bearing encephalitogenic peptides induce T-cell tolerance and ameliorate experimental autoimmune encephalomyelitis. *Nat Biotechnol* 30(12):1217–1224.
14. Getts DR, et al. (2014) Therapeutic inflammatory monocyte modulation using immune-modifying microparticles. *Sci Transl Med* 6(219):219ra217.
15. Kontos S, Kourtis IC, Dane KY, Hubbell JA (2013) Engineering antigens for in situ erythrocyte binding induces T-cell deletion. *Proc Natl Acad Sci USA* 110(1):E60–E68.
16. Irvine DJ, Swartz MA, Szeto GL (2013) Engineering synthetic vaccines using cues from natural immunity. *Nat Mater* 12(11):978–990.
17. Tsai S, et al. (2010) Reversal of autoimmunity by boosting memory-like autoregulatory T cells. *Immunity* 32(4):568–580.
18. Macauley MS, et al. (2013) Antigenic liposomes displaying CD22 ligands induce antigen-specific B cell apoptosis. *J Clin Invest* 123(7):3074–3083.
19. Yeste A, Nadeau M, Burns EJ, Weiner HL, Quintana FJ (2012) Nanoparticle-mediated codelivery of myelin antigen and a tolerogenic small molecule suppresses experimental autoimmune encephalomyelitis. *Proc Natl Acad Sci USA* 109(28):11270–11275.
20. Joseph A, Munroe K, Housman M, Garman R, Richards S (2008) Immune tolerance induction to enzyme-replacement therapy by co-administration of short-term, low-dose methotrexate in a murine Pompe disease model. *Clin Exp Immunol* 152(1):138–146.
21. Steinman RM, Hawiger D, Nussenzweig MC (2003) Tolerogenic dendritic cells. *Annu Rev Immunol* 21:685–711.
22. Maldonado RA, von Andrian UH (2010) How tolerogenic dendritic cells induce regulatory T cells. *Adv Immunol* 108:111–165.
23. Thomson AW (2010) Tolerogenic dendritic cells: All present and correct? *Am J Transplant* 10(2):214–219.
24. Manicassamy S, Pulendran B (2011) Dendritic cell control of tolerogenic responses. *Immunol Rev* 241(1):206–227.
25. Cobbold SP, Adams E, Nolan KF, Regateiro FS, Waldmann H (2010) Connecting the mechanisms of T-cell regulation: Dendritic cells as the missing link. *Immunol Rev* 236:203–218.
26. Taner T, Hackstein H, Wang Z, Morelli AE, Thomson AW (2005) Rapamycin-treated, alloantigen-pulsed host dendritic cells induce ag-specific T cell regulation and prolong graft survival. *Am J Transplant* 5(2):228–236.
27. Fischer R, Turnquist HR, Taner T, Thomson AW (2009) Use of rapamycin in the induction of tolerogenic dendritic cells. *Handb Exp Pharmacol* (188):215–232.
28. Powell JD, Pollizzi KN, Heikamp EB, Horton MR (2012) Regulation of immune responses by mTOR. *Annu Rev Immunol* 30:39–68.
29. Araki K, Ellebedy AH, Ahmed R (2011) TOR in the immune system. *Curr Opin Cell Biol* 23(6):707–715.
30. Bachmann MF, Jennings GT (2010) Vaccine delivery: A matter of size, geometry, kinetics and molecular patterns. *Nat Rev Immunol* 10(11):787–796.
31. Metcalfe SM, Fahmy TM (2012) Targeted nanotherapy for induction of therapeutic immune responses. *Trends Mol Med* 18(2):72–80.
32. Look M, et al. (2013) Nanogel-based delivery of mycophenolic acid ameliorates systemic lupus erythematosus in mice. *J Clin Invest* 123(4):1741–1749.
33. Goodnow CC, et al. (1988) Altered immunoglobulin expression and functional silencing of self-reactive B lymphocytes in transgenic mice. *Nature* 334(6184):676–682.
34. Vasquez KO, Casavant C, Peterson JD (2011) Quantitative whole body biodistribution of fluorescent-labeled agents by non-invasive tomographic imaging. *PLoS ONE* 6(6):e20594.
35. Liu E, et al. (2002) Anti-peptide autoantibodies and fatal anaphylaxis in NOD mice in response to insulin self-peptides B:9-23 and B:13-23. *J Clin Invest* 110(7):1021–1027.
36. Krieckaert C, Rispens T, Wolbink G (2012) Immunogenicity of biological therapeutics: From assay to patient. *Curr Opin Rheumatol* 24(3):306–311.
37. Vultaggio A, Maggi E, Matucci A (2011) Immediate adverse reactions to biologicals: From pathogenic mechanisms to prophylactic management. *Curr Opin Allergy Clin Immunol* 11(3):262–268.
38. Qian J, Borovok M, Bi L, Kazazian HH, Jr, Hoyer LW (1999) Inhibitor antibody development and T cell response to human factor VIII in murine hemophilia A. *Thromb Haemost* 81(2):240–244.
39. Selecta Biosciences (2011) *Safety and Pharmacodynamics of SEL-068 Vaccine in Smokers and Non-Smokers*. Available at www.ClinicalTrials.gov.
40. Araki K, et al. (2009) mTOR regulates memory CD8 T-cell differentiation. *Nature* 460(7251):108–112.
41. Smarr CB, Bryce PJ, Miller SD (2013) Antigen-specific tolerance in immunotherapy of Th2-associated allergic diseases. *Crit Rev Immunol* 33(5):389–414.
42. Scott DW, Pratt KP, Miao CH (2013) Progress toward inducing immunologic tolerance to factor VIII. *Blood* 121(22):4449–4456.
43. Enever C, Batuwangala T, Plummer C, Sepp A (2009) Next generation immunotherapeutics—Honing the magic bullet. *Curr Opin Biotechnol* 20(4):405–411.
44. Astete CE, Sabliov CM (2006) Synthesis and characterization of PLGA nanoparticles. *J Biomater Sci Polym Ed* 17(3):247–289.
45. Bi L, et al. (1995) Targeted disruption of the mouse factor VIII gene produces a model of haemophilia A. *Nat Genet* 10(1):119–121.
46. Bailón E, et al. (2012) A shorter and more specific oral sensitization-based experimental model of food allergy in mice. *J Immunol Methods* 381(1-2):41–49.
47. Kasper CK, et al. (1975) Proceedings: A more uniform measurement of factor VIII inhibitors. *Thromb Diath Haemorrh* 34(2):612.

Supporting Information

Maldonado et al. 10.1073/pnas.1408686111

SI Materials and Methods

Proteins and Reagents. $FVIII_{75–89}$ (VHLFNIAKPRPPWMG), $FVIII_{1723–1737}$ (ERLWDYGMSSSPHVL), and $FVIII_{2210–2229}$ (TASSYFTNMFATWSPSKAR) were synthesized by Anaspec. Ovalbumin (OVA) and HEL (Worthington Biochemical Corporation), $OVA_{323–339}$ peptide (Bachem Americas, Inc.), $PLP_{139–151}$ peptide (US Biological Life Sciences), aluminum hydroxide gel (Alum) (Sigma and Invivogen), and cholera toxin (List Biological Laboratories) were purchased from the suppliers indicated. Anti-CD11c (HL-3, N418), anti-EMR1 (F4/80), anti-CD8α (53-6.7), anti-CD45R (RA3-6B2), anti-CD4 (GK1.5), and anti-CD25 (PC61) antibodies were purchased from BD Biosciences. Anti-Foxp3 (FJK-16s), anti-Ki67 (SolA15), 7AAD, and anti-CD11b (M1/70) antibodies were purchased from eBiosciences. Anti-CD19 (6D5), TCRVa2 (B20.1), TCRb (H57-597), CD38 (90), IgD (11-26c.2a), GL7 (GL7), Ki67 (SolA15, eBio), 7AAD (eBio), Gr1 (RB6-8C5), F4/80 (BM8), and anti-IL10 (JES5-16E3) were purchased from Biolegend.

Generation of pOVA. Chicken OVA protein was dissolved in PBS. The solution pH was raised to 12 by adding 3 M of NaOH, and then the pH was lowered to 2 using trifluoracetic acid to coacervate the protein. This pH cycling was repeated three additional times, and then the solution pH was raised to 7 using 3 M of NaOH. The coacervated protein was then homogenized three times at 20,000 psi using a Microfluidics LV1 microfluidizer with G10Z interaction chamber to reduce the particle size to ~200 nm as determined by dynamic light scattering (DLS).

Mice and Mouse Cells. C57/BL6, Balb/C, OTII+, and OTII+ $RAG1^{-/-}$ mice were obtained from Jackson Laboratories or Taconic Farms. When indicated, T and B cells were isolated from single-cell suspensions of LNs and/or spleens of young mice and enriched using magnetic sorting (MACS, Miltenyi). In some cases, T cells were labeled with carboxyfluorescein diacetate succinimidyl diester (CFSE, Invitrogen) by incubation for 10 min at 37 °C with CFSE in RPMI medium containing 10% FCS to trace their proliferation in vitro (1 μM) or in vivo (10 μM). FVIII-deficient hemophilia A mice (1) (E16, C57BL/6 background) were maintained in the animal facility of the Uniformed Services University of the Health Sciences.

ELISA. The levels of anti-OVA IgG antibodies were measured by ELISA. Briefly, assay plates (Costar 9017 96-well flat-bottom plates) were coated with 100 μL of OVA protein (5 μg/mL, Worthington Biochemical LS003054) and incubated overnight at 4 °C. Plates were washed with 0.05% Tween-20 in PBS and then blocked with casein in PBS. Assay wells were washed, and serial dilutions of samples were added and incubated at room temperature for 2 h. Anti-OVA antibody was detected by addition of HRP-conjugated goat anti-mouse anti-IgG (AbCam ab98717) followed by addition of substrate (BD Biosciences TMB Substrate Reagent Set, catalog no. 555214). The optical density (OD) of the wells was assessed immediately after adding the stop solution on a plate reader at wavelengths of 450 nm with subtraction at 570 nm. Data analysis was performed using Molecular Device's software SoftMax Pro v6.2.2. A four-parameter logistic curve-fit graph was prepared with the dilution on the x axis (log scale) and the OD value on the y axis (linear scale), and the half maximum value (EC_{50}) for each sample was determined.

The KLH ELISA followed a similar protocol but used Maxisorp assay plates (NUNC 44-2404-21) and a coating of KLH (Sigma H7127) at 5 μg/mL. The anti-OVA IgE titers were determined using a sandwich ELISA. The Costar plates were coated with anti-mouse IgE (AbD Serotec MCA419) and incubated overnight. Samples were serially diluted and added to blocked wells for 2 h. Samples were detected with biotin-conjugated rabbit anti-OVA IgG (AbCam ab8389) followed by streptavidin–HRP (BD 554066).

mMCP-1 concentrations were determined using Affymetrix Mouse MCPT-1 ELISA Kit (88-7503-88).

Assays for Anti-FVIII Antibody Levels and Inhibitor Titers. Anti-FVIII antibody levels were determined by ELISA. ELISA plates were coated with 1 μg/mL of recombinant FVIII (rFVIII) overnight at 4 °C. For quantification, a standard curve was generated with a mixture of monoclonal anti-FVIII A2 and C2 antibodies.

The FVIII inhibitor titer was determined by Bethesda assay using a previously published protocol with minor modification (2). The inhibitor titer was established from a semilogarithmic plot of residual FVIII activity (logarithmic) and units of inhibitor activity (linear) (2). The dilution of test plasma giving a residual FVIII activity of 50% is said to contain one Bethesda unit FVIII inhibitor activity per milliliter.

Immunizations. Three major modalities of immunizations were used: OVA(25 μg)+CpG (20 μg) s.c. in the hind limbs or front limbs, pOVA (10 μg) intravenously, KLH (50 μg) s.c. in the base tail (50 μg) or the front limbs (50 μg), OVA (5 mg) with cholera toxin (CTx, 10μg) weekly, and the aforementioned OVA+Alum.

BALB/c female mice aged 8–10 wk were administered 5 mg of OVA with 10 μg of CTx (List Biologicals) weekly. In animals immunized with OVA+CpG on days 0, 14, and 28, a delayed-type hypersensitivity response was evaluated by injecting one hind limb with PBS and the other with 10 μg of OVA. The following day, the two limbs were measured with a caliper to determine the degree of inflammation. In other instances, repetitive infusions with pOVA i.v. led to anaphylaxic reactions that were scored by three blinded scorers as previously described (3): 0, no symptom; 1, lethargy; 2, lethargy and inability to right; 3, moribund.

1. Bi L, et al. (1995) Targeted disruption of the mouse factor VIII gene produces a model of haemophilia A. *Nat Genet* 10(1):119–121.
2. Kasper CK, et al. (1975) Proceedings: A more uniform measurement of factor VIII inhibitors. *Thromb Diath Haemorrh* 34(2):612.
3. Liu E, et al. (2002) Anti-peptide autoantibodies and fatal anaphylaxis in NOD mice in response to insulin self-peptides B:9-23 and B:13-23. *J Clin Invest* 110(7):1021–1027.

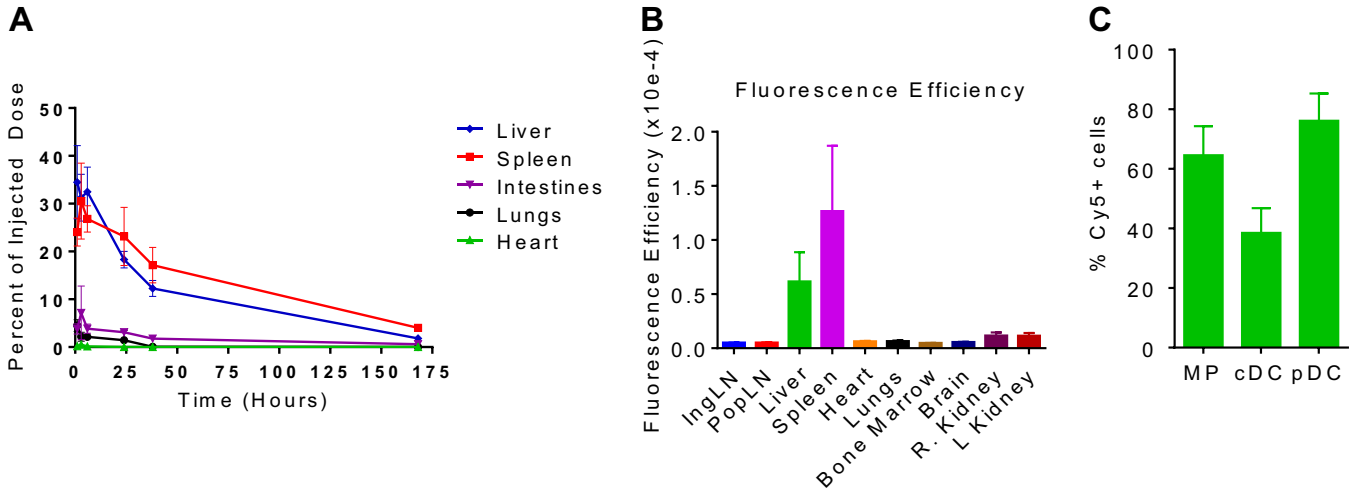

Fig. S1. Biodistribution of fluorescently labeled NPs. (*A*) Balb/C animals were immunized with pOVA on days −27 and −13 before the injection of NPs. On day 0, fluorescently tagged Cy7–tNPs were injected i.v. in in vivo whole animal with imaging by FMT. Mice were subjected to imaging on a FMT instrument. Fluorescence signal was quantified at 1, 3, 6, 24, and 48 h ($n = 3$) and at 168 h ($n = 1$) after injection for selected organs. (*B*) Ex vivo analysis of tNP biodistribution. Animals were killed at 48 h ($n = 2$), and selected organs were harvested and analyzed for fluorescence signal. (*C*) Cellular localization of NP in the spleen. Animals were injected i.v. with tNP (containing rapamycin+OVA) labeled with Cy5. Spleen cells were harvested the next day and macrophages (MPs; F4/80+CD11b+Gr1−), conventional DC (cDC; MHCCLII+CD11c+CD11b+), and plasmacytoid DC (pDC; MHCCLII+CD11c+B220+PDCA1+) were analyzed by flow cytometry ($n = 3$ per group).

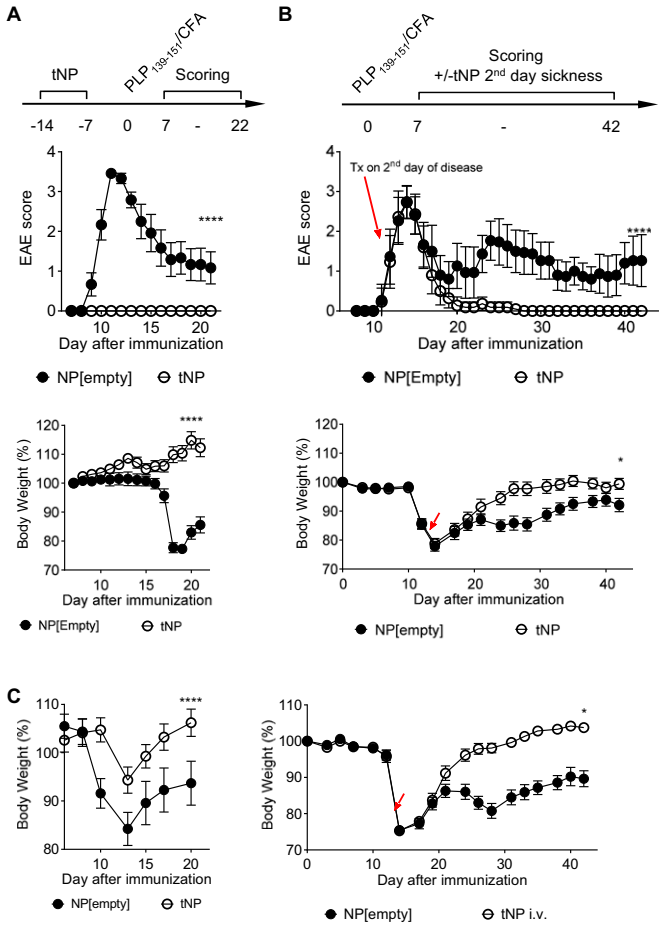

Fig. S2. Induction of tolerance in R-EAE using tNP. (*A*) Prophylactic treatment. SJL mice ($n = 12$) were treated prophylactically with two injections of tNP loaded with $PLP_{139–151}$ and rapamycin or with placebo NPs (empty NP) on days −14 and −7. R-EAE was induced on day 0 by injection of $PLP_{139–151}$ emulsfied in CFA followed by pertussis toxin (PTx). Disease was scored by blinded observers. (*B*) Therapeutic treatment. R-EAE in SJL mice ($n = 15$) was induced on day 0 by s.c. administration of $PLP_{139–151}$/CFA. Animals were individually monitored for onset of disease and treated on the second day of detectable disease (score ≥ 1, around day 12) with either empty NP or tNP. Body weight of animals was measured three times per week. The results are represented as the mean ± 95% confidence interval. For statistical analysis, Student *t* test with two-tailed distribution was used (****$P < 0.0001$). (*C*) Body weight measurements in EAE. Mice described in Fig. 6 *A* and *B* were monitored for body weight three times per week (*Left* and *Right* panels, respectively). The results are represented as the mean ± 95% confidence interval. For statistical analysis, Student *t* test with two-tailed distribution was used (****$P < 0.0001$).